Author Manuscript

Author Manuscript

Author Manuscript

Author Manuscript

HHS Public Access

Author manuscript

Neuroimage. Author manuscript; available in PMC 2023 November 28.

Published in final edited form as:

Neuroimage. 2020 October 15; 220: 117062. doi:10.1016/j.neuroimage.2020.117062.

Longitudinal analysis of regional cerebellum volumes during normal aging

Shuo Han[a,b,*], **Yang An**[b], **Aaron Carass**[c,d], **Jerry L. Prince**[a,c,d], **Susan M. Resnick**[b]

[a]Department of Biomedical Engineering, The Johns Hopkins University, Baltimore, MD, 21218, USA

[b]Laboratory of Behavioral Neuroscience, National Institute on Aging, National Institutes of Health, Baltimore, MD, 20892, USA

[c]Department of Electrical and Computer Engineering, The Johns Hopkins University, Baltimore, MD, 21218, USA

[d]Department of Computer Science, The Johns Hopkins University, Baltimore, MD, 21218, USA

Abstract

Some cross-sectional studies suggest reduced cerebellar volumes with aging, but there have been few longitudinal studies of age changes in cerebellar subregions in cognitively healthy older adults. In this work, 2,023 magnetic resonance (MR) images of 822 cognitively normal participants from the Baltimore Longitudinal Study of Aging (BLSA) were analyzed. Participants ranged in age from 50 to 95 years (mean 70.7 years) at the baseline assessment. Follow-up intervals were 1–9 years (mean 3.7 years) for participants with two or more visits. We used a recently developed cerebellum parcellation algorithm based on convolutional neural networks to divide the cerebellum into 28 subregions. Linear mixed effects models were applied to the volume of each cerebellar subregion to investigate cross-sectional and longitudinal age effects, as well as effects of sex and their interactions, after adjusting for intracranial volume. Our findings suggest spatially varying atrophy patterns across the cerebellum with respect to age and sex both cross-sectionally and longitudinally.

Keywords

Cerebellum; Normal aging; Longitudinal analysis

This is an open access article under the CC BY-NC-ND license (http://creativecommons.org/licenses/by-nc-nd/4.0/).

[*]Corresponding author. Department of Biomedical Engineering, The Johns Hopkins University, 3400 N. Charles St., Baltimore, MD, 21218, USA. shan50@jhu.edu (S. Han).

CRediT authorship contribution statement

Shuo Han: Software, Validation, Formal analysis, Data curation, Writing - original draft, Visualization. **Yang An:** Conceptualization, Methodology, Data curation, Writing - review & editing. **Aaron Carass:** Writing - review & editing. **Jerry L. Prince:** Writing - review & editing, Supervision. **Susan M. Resnick:** Conceptualization, Methodology, Investigation, Resources, Supervision, Funding acquisition, Writing - review & editing, Project administration, Resources.

Appendix A. Supplementary data

Supplementary data to this article can be found online at https://doi.org/10.1016/j.neuroimage.2020.117062.

Author Manuscript Author Manuscript Author Manuscript Author Manuscript

1. Introduction

Previous studies have shown that spatial locations within the cerebellum relate to specific motor and cognitive functions (Mottolese et al., 2013; Stoodley and Schmahmann, 2018; Guell et al., 2018; Schmahmann, 2019). For example, in the functional magnetic resonance image analysis by Guell et al. (2018), activation during performance of motor tasks was found in Lobules IV, V, VI, and VIII, while activation during performance of cognition tasks were found in Lobules VI, Crus I, Crus II, VIIB, IX, and X. Since different functions exhibit different trajectories of change during aging (Tian et al., 2017; Goh et al., 2012) and across men and women (McCarrey et al., 2016), it is of interest to characterize regional changes of the cerebellum in cognitively normal individuals during aging.

By parcellating the cerebellum into its subregions using structural magnetic resonance (MR) images, previous studies have shown age and sex differences in cerebellar regional volumes. Luft et al. (1999) used a semi-automated method to parcellate the cerebellum into 11 regions for 48 subjects. Age effects on volumes were found in Vermis, and Vermis VI–VII and medial Superior Posterior Lobe were found larger for women than men when adjusting for the intracranial volume (ICV). Bernard and Seidler (2013) used an automatic algorithm, SUIT (Diedrichsen et al., 2009), to parcellate the cerebellum into 27 regions, and group differences were analyzed for two populations with distinct age distributions. Eleven regions were found significantly different for those two groups when adjusted for ICV. In another study (Bernard et al., 2015), the authors analyzed a set of 123 subjects from 12 to 65 years old. Parcellation with SUIT was performed but statistical results were provided only for seven combined regions. They showed that the volumes of different regions were best fitted with respect to age using different functions such as logarithmic, linear, and quadratic functions, but the effects of sex were not studied quantitatively. Koppelmans et al. (2017) also used SUIT to parcellate the cerebellum and then combined subregions into 11 regions for 213 subjects. Age effects were found for 8 regions when adjusting for sex and ICV. In summary, Luft et al. (1999) and Koppelmans et al. (2017) both found a reduced volume in the vermis with older age. Bernard and Seidler (2013) and Koppelmans et al. (2017) found reduced volumes of bilateral Crus I with older age. Results for other subregions vary across studies and are hard to compare due to use of different regional definitions. In addition to cross-sectional studies, Raz et al. (2013, 2010, 2005, 2003) conducted longitudinal analyses on the cerebellum and found shrinkage over time, but they focused on the cerebellar hemispheres. Related studies examining age effects on subregional cerebellar volumes in cognitively healthy individuals are summarized in Table 1.

It is evident that previous studies on cerebellar subregional volumes are limited in either the sample size of cognitively normal older subjects or the number of parcellated regions. Furthermore, since the majority of studies are cross-sectional, the analyses describe between-subject variation, or age differences, rather than intra-individual changes from longitudinal analysis where the same subject underwent multiple visits. In this work, we conducted longitudinal analysis of the regional cerebellum volumes during normal aging for 822 non-demented participants with 2,023 magnetization-prepared rapid gradient-echo (MPRAGE) images from the Baltimore Longitudinal Study of Aging (BLSA) (Shock et al., 1984). A recent cerebellum parcellation algorithm based on convolutional neural networks

Author Manuscript Author Manuscript Author Manuscript Author Manuscript

(Han et al., 2019) was used to parcellate the cerebellum into 28 regions which were further grouped into three additional levels according to the anatomical hierarchies of the cerebellum (Schmahmann et al., 2000; Carass et al., 2018). The results then underwent visual inspection before inclusion in the current study. Our longitudinal analyses answer the following questions related to cerebellar volumes including subregions in older adults: cross-sectional effects of age and sex, longitudinal changes, and whether age and sex modify the longitudinal changes.

2. Methods

2.1. Participants

The Baltimore Longitudinal Study of Aging (BLSA) is an observational study that began in 1958 and is currently conducted by the National Institute on Aging Intramural Research Program (Shock et al., 1984). Recruitment is ongoing, and participants and visits included in these analyses represent a snapshot in time. The current visit schedule depends on age: participants younger than 60 are assessed every 4 years, participants between 60 and 80 are assessed every 2 years, and participants older than 80 are assessed every year. The varied numbers of visits per participant primarily reflect the timing of enrollment and their age. 2,381 available MPRAGE images for 1,017 participants were processed. 70 images with artifacts or low parcellation quality were excluded, as summarized in Table 2. We excluded 98 images for visits after the year of onset of dementia or mild cognitive impairment (MCI) (Armstrong et al., 2019). Due to very limited longitudinal data in younger participants in BLSA, we focused this study on subjects older than 50 years, resulting in 2,033 images. The intracranial volume (ICV) was calculated using a brain extraction algorithm, MASS (Doshi et al., 2013), from a separate study. We used the ICV value from the earliest visit for each subject, and 10 subjects without ICV were excluded. The final dataset included 2,023 images from 822 subjects. The mean age at baseline is 70.7 years with standard deviation (SD) 10.2 years. The mean follow-up interval for subjects with multiple visits is 3.7 years with SD 1.9 years. These subjects are highly educated (17.0 years of education on average) and mostly Caucasian (67.5%). The demographic characteristics of the participants are further summarized in Table 3.

2.2. MRI acquisition and image analysis

The images were acquired on 3.0 T MR scanners (Achieva, Phillips Medical Systems, Netherlands). Image matrix = 256 × 240, number of sagittal slices = 170, pixel size = 1mm × 1mm, slice thickness = 1.2 mm, flip angle = 8°, echo time (TE) = 3.1 ms, 47 images were acquired with repetition time (TR) = 6.8 ms, and 1,976 images were acquired with TR = 6.6 ms.

A cerebellum parcellation algorithm based on convolutional neural networks (Han et al., 2019) was applied to all images. A brief overview of this algorithm is as follows. The images were inhomogeneity-corrected using N4 (Tustison et al., 2010) and rigidly registered to the 1 mm isotropic ICBM 2009c template (Fonov et al., 2011) in MNI space using the ANTs registration suite [1]. The parcellation classifiers trained from 15 expert manual delineations (the Adult Cohort in Carass et al. (2018)) were used to perform per-voxel

Author Manuscript Author Manuscript Author Manuscript Author Manuscript

labeling, and small, isolated pieces were removed in post-processing. This algorithm resulted in 28 cerebellar regions: bilateral Lobules I–III, IV, V, and VI; Crus I and II; Lobules VIIB, VIIIA, VIIIB, IX, and X; Vermis VI, VII, VIII, IX, and X; and Corpus Medullare (CM). Since some previous methods report statistical analysis of coarser levels of cerebellar divisions (Luft et al., 1999; Raz et al., 2013; Koppelmans et al., 2017), we also provide results of anatomically meaningful grouped regions (Schmahmann et al., 2000) in addition to subcomponents, so as to facilitate more direct comparisons among the literature. Following Schmahmann et al. (2000), these regions were grouped into bilateral Anterior, Posterior, and Flocculonodular Lobes, Vermis VI–VII, VIII–IX, and X, and further into bilateral hemispheres, the whole Vermis, and the whole cerebellum. Finally, the volumes of each region at each grouping level were calculated.

In addition to the cross-validation study included in Han et al. (2019), we also calculated intraclass correlations (ICC) for each of the cerebellar regions to validate this algorithm. The ICCs were calculated using linear mixed-effects models. The fixed effects included intercept and age while the random effects included only the intercept, and the data were grouped by subjects. The ICC is defined as

$$\mathrm{ICC} = \frac{\sigma_1^2}{\sigma_1^2 + \sigma_0^2}, \tag{1}$$

where σ_1^2 is the variance of intercept in random effects and σ_0^2 is the variance of residuals. ICCs of the 28 cerebellum regions ranging from 0.87 to 0.99 are shown in Table 4. ICCs in the rang [0.75–0.90) are considered good and values [0.90–1.00] are considered excellent (Koo and Li, 2016). In summary, this equates to 25 of our cerebellum regions as excellent and the remaining three as good.

2.3. Statistical analysis

Linear mixed-effects regressions were used to study the relationship of age and sex with baseline and longitudinal change in each cerebellar volume individually. There are 28 lobular regions from the parcellation algorithm plus 9 grouped regions, resulting in 37 regions in total (see Table 5 for results). The volume in mm^3 of each of these regions was used as a separate outcome in each of the 37 regressions. The fixed effects are intercept, ICV in cm^3 centered around 1,400, baseline age in years centered around 70, sex with 0.5 indicating male and — 0.5 indicating female, follow-up interval in years, the interaction between baseline age and follow-up interval (baseline age × follow-up interval), and the interaction between sex and follow-up interval (sex × follow-up interval). The random effects are intercept and follow-up interval. To account for multiple comparisons, p-values of each fixed effect were adjusted across the 37 regions using Bonferroni correction. Type I error level $p \leq 0.05$ was applied to the adjusted p-values to test whether the fixed effects are significantly different from 0. All linear mixed-effects models were fit in R version 3.5.1 using lme function from nlme library version 3.1.137 (Pinheiro et al., 2019).

[1] http://stnava.github.io/ANTs/.

Author Manuscript Author Manuscript Author Manuscript Author Manuscript

3. Results

The estimated coefficients, standard errors, and raw p-values of baseline age, sex, follow-up interval, and the interactions for each cerebellar region are shown in Table 5. Significant effects for Bonferroni adjusted $p \leq 0.05$ of each region are highlighted.

3.1. Total cerebellum, Corpus Medullare, and hemispheres

Both baseline age and follow-up interval are significant for the total cerebellum, CM, and bilateral hemispheres, indicating that volumes are smaller with higher age and decline longitudinally. The interaction between baseline age and follow-up interval is significant for the total cerebellum and Left Hemisphere. Negative coefficients suggest that the volumes decline faster at more advanced baseline age. Sex is not significant for any of these regions. The interaction between sex and follow-up interval is significant for CM, suggesting that the volume declines faster for men.

3.2. Vermis and lobules

Baseline age, follow-up interval, and the interaction between these two factors are significant for the whole Vermis, suggesting that the Vermis volume is smaller at higher baseline age and declines longitudinally over time, and this decline is faster at higher baseline age.

For the subregions of Vermis, baseline age and follow-up interval are significant for Vermis VI–IX (the part corresponding to Posterior Lobe) and its sub-regions Vermis VI and IX, suggesting smaller volumes at higher age and longitudinal declines over time. The interaction between baseline age and follow-up interval is significant for the Vermis VI–IX and its sub-region Vermis VI, suggesting faster declines at more advanced baseline age. Sex is significant for Vermis IX and Vermis X (the part corresponding to Flocculonodular Lobe) with negative coefficients, suggesting smaller volumes for men than women.

3.3. Anterior lobe and lobules

Both baseline age and follow-up interval are significant for Right Anterior Lobe, indicating that its volume is smaller with higher age and declines longitudinally over time. The interaction between baseline age and follow-up time is significant for both sides, indicating faster declines at higher baseline age. There is no significant sex difference but there is a significant interaction between sex and follow-up interval for Left Anterior Lobe. This interaction shows less steep decline in men compared with women at advanced age.

For lobules of the Anterior Lobe, baseline age is significant for Right Lobules I–III and bilateral Lobules V, indicating smaller volumes with higher age. Sex is significant for Right Lobules I–III, suggesting that the volume is greater for women than men at baseline. Longitudinal change is significant for all lobules of Anterior Lobe. Note that the coefficient of follow-up interval for bilateral Lobules IV is positive, indicating increasing volumes over time. The interaction between baseline age and follow-up interval is significant for Right Lobule IV, suggesting a steeper decline at more advanced baseline age.

Author Manuscript Author Manuscript Author Manuscript Author Manuscript

3.4. Posterior Lobe and lobules

Baseline age and follow-up interval are significant for the bilateral Posterior Lobes, suggesting that the volumes are smaller with higher baseline age and decline longitudinally. Sex is not significant for the Posterior Lobe.

For lobules of the Posterior Lobe, baseline age is significant for all lobules except for bilateral Lobule VIIIA, suggesting smaller volumes with higher baseline age. Sex is significant for bilateral Lobules VIIIA with positive coefficients, indicating larger volumes for men at baseline. Follow-up interval is significant except for Right VIIIA, suggesting longitudinal declines over time. The interaction between sex and follow-up interval is significant for Right Crus II with a negative coefficient, suggesting a faster decline for men than women.

3.5. Flocculonodular Lobes

Flocculonodular Lobe is only composed of Lobule X. Baseline age is significant for bilateral Lobules X, indicating smaller volumes at higher baseline age. Follow-up interval is significant for the left, indicating a longitudinal decline over time. The interaction between baseline age and follow-up interval is significant for the right, indicating a steeper decline at higher baseline age.

3.6. Visualization

To visualize the results, we further show the fitted population average trajectories for CM, Vermis VI–IX and X, and Anterior, Posterior, and Flocculonodular Lobes (Flocculonodular Lobe is only composed of Lobule X) in Fig. 1. Since we observed similar age differences and age changes for the bilateral regions, we summed their volumes together before performing the regressions only for visualization purposes. To plot the curves, we used baseline age from 55 to 90 in 5-year age bands, follow-up intervals from 0 to 4 years for each baseline age, and ICV 1,400 cm^3, by sex. Note that if the coefficients of the interactions—baseline age × follow-up interval and sex × follow-up interval—are not significant, we do not incorporate them into this figure. Additional plots are shown in the supplementary materials. The color-coded raw p values of baseline age, sex, and follow-up interval on top of a cerebellum illustration are further shown in Fig. 2.

4. Discussion

In this work, we analyzed age differences and longitudinal changes of cerebellar regional volumes in a large sample of non-demented individuals with baseline age 50 years and older. Our results indicate that the cerebellum volume has spatially varying trajectories with respect to baseline age and longitudinal change over time and only a few subregions show sex differences after adjustment for ICV. Twenty of the 28 parcellated regions (cerebellar lobules and CM) show statistically significant cross-sectional age effects. Twenty-three of the 28 regions have statistically significant longitudinal changes. For three of the 28 regions, longitudinal volume loss is greater with advancing baseline age. Five of the 28 regions show statistically significant sex effects at baseline, and men compared with women showed greater longitudinal volume loss in three regions.

Author Manuscript Author Manuscript Author Manuscript Author Manuscript

We used a cerebellum parcellation algorithm based on convolutional neural networks in this work (Han et al., 2019). Compared with previous methods, such as SUIT (Diedrichsen et al., 2009), which was used by Bernard and Seidler (2013), Bernard et al. (2015) and Koppelmans et al. (2017), and MAGet Brain (Park et al., 2014), which was used by Steele and Chakravarty (2018), our parcellation algorithm has two advantages. First, our algorithm is fully-automatic, and takes approximately a minute to parcellate a cerebellum (without considering image pre-processing such as intensity inhomogeneity correction (Tustison et al., 2010) and MNI space alignment (Fonov et al., 2011)). In comparison, SUIT requires manual intervention and takes about 10 min to parcellate a cerebellum image; although MAGeT Brain is fully-automatic, it takes approximately 6 h for parcellation (Park et al., 2014). These features enable us to process thousands of images in a reasonable amount of time. Second, our algorithm has better parcellation accuracy compared with previous methods (Han et al., 2020; Carass et al., 2018; Romero et al., 2017). A disadvantage of our parcellation algorithm is that it is sensitive to image contrast. Therefore, we only analyzed MPRAGE images despite also having images acquired with the spoiled gradient echo sequence. Similar to SUIT and MAGeT Brain, the definition of cerebellar regions in our algorithm is based on Schmahmann et al. (2000). However, SUIT and MAGet Brain provide more detailed divisions of the vermis compared to our algorithm, while our algorithm provides more detailed divisions of the anterior lobe than SUIT.

The main benefit of longitudinal analyses is the ability to investigate intra-individual changes over time, i.e. longitudinal changes of the cerebellar subregions, and the effects of inter-individual differences on the intra-individual changes, i.e. whether baseline age and sex modify the longitudinal changes in total and subregional cerebellar volumes. Our analyses extend prior findings that investigate inter-individual differences based on cross-sectional analyses or findings of longitudinal changes that are restricted to total or hemispheric cerebellar volumes. Linear mixed-effects models use all available data to estimate longitudinal trajectories. Different subjects can have a different number of visits, i.e. unbalanced data. One of the strengths of the linear mixed-effects model is the ability to appropriately handle such unbalanced data. In addition to subjects with multiple visits, we also included subjects with only one visit. These data would mainly contribute to the cross-sectional effects in our linear mixed-effect models, so excluding them from the analysis will yield similar results for the longitudinal effects. However, the advantage of including participants with a single visit is to improve power for estimation of cross-sectional effects. We used Bonferroni correction to account for multiple comparisons. However, because our regions are correlated, the hypotheses are correlated as well. Since commonly used approaches to correct for multiple comparisons, including Bonferroni and false discovery rate corrections, do not fully account for these correlations (Bretz et al., 2011), the adjusted p-values are too conservative. Unfortunately, alternatives such as permutation and bootstrapping remain challenging to apply in linear mixed effects models (Joo et al., 2016). This limitation could be investigated in the future.

In contrast to previous work, we conducted longitudinal analyses of a hierarchy of cerebellar subregions—cerebellar lobules, lobes, and hemispheres—of non-demented subjects in this age range. Most previous work of cerebellar subregions was based on cross-sectional analysis (Luft et al., 1999; Bernard and Seidler, 2013; Bernard et al., 2015; Koppelmans

Author Manuscript Author Manuscript Author Manuscript Author Manuscript

et al., 2017; Steele and Chakravarty, 2018). To our knowledge, the single publication of subregional longitudinal analysis of the cerebellum (Tiemeier et al., 2010) focused on cerebellum development in children and adolescence. The work by Raz et al. (2013, 2010, 2005, 2003) also conducted longitudinal analysis but focused on cerebellum hemispheres instead of lobular regions. In terms of the cross-sectional differences—baseline age and sex—our results are not entirely in agreement with previous work. Bernard and Seidler (2013) found significant age differences for the volumes of bilateral Lobules I–IV, V, and VI, bilateral Crus I, Left Crus II, Vermis VI, and Vermis VIIB. However, we do not find significant age differences in Left Lobules I–III, bilateral Lobules IV, or Vermis VII, and we find significant age differences in many other regions, perhaps due to greater sample size. Bernard et al. (2015) modeled the volumes of Vermis and bilateral Anterior Lobes using logarithmic fits, bilateral Crus I using linear fits, and Posterior Lobes using quadratic fits. They further showed that females and males could be modeled using different fits for these regions. However, we do not find the coefficient of baseline age is significantly different from zero for the left Anterior Lobe in our study, and their results with respect to sex are not directly comparable to ours since they did not statistically analyze the differences between the two sexes. Koppelmans et al. (2017) analyzed the volumes of bilateral Lobules I–VI, Crus I, Crus II–Lobules VIIB, Lobules VIIIB–IX, Lobules X, and Vermis, and found significant age differences except for right Crus II–Lobules VIIB and bilateral Lobules X. In contrast, we find significant age differences in right Crus II, right Lobule VIIB, and bilateral Lobules X, and we do not find significant age difference in Left Lobules I–III or bilateral Lobule IV. Steele and Chakravarty (2018) found that bilateral Crus II and Vermis VI are larger for women, while right Lobule V, bilateral Lobules VIIIA and VIIIB, and Vermis VIIIA and VIIIB are larger for men after dividing each region by the volume of total cerebellar gray matter. In contrast, we incorporated ICV as a covariate in our regressions, and we find no significant sex differences for bilateral Crus II, Vermis VI, Right Lobule V, bilateral Lobules VIIIB, and Vermis VIII. Consistent with findings of Steele and Chakravarty (2018), we find that bilateral Lobules VIIIA are significantly larger for men. Additionally, we find significant sex differences in Right Lobules I–III, and Vermis IX and X. Note that we found significant increasing volumes of bilateral Lobules IV over time. Whether it is physiologically meaningful or the result of noise from the parcellation algorithm is unclear at present; further investigation is warranted.

Given that this study is the largest study of its nature, it is tempting to see this work as the definitive "*Atlas of the Aging Cerebellum*". We, however, caution that our findings are not consistent with some of the earlier work in the literature. We are still in the discovery phase when it comes to understanding the (aging) cerebellum. We also note that our study differs from prior work with respect to region definition, statistical analysis, and study sample. In addition, our results may lack generalizability because the subjects are highly educated and mostly Caucasian. The imaging visits included in these analyses were restricted to those where participants remained free of cognitive impairment. Future work can investigate whether acceleration of regional cerebellum loss occurs in individuals who ultimately develop cognitive impairment. Future work can also include analysis of the relationships between regional cerebellum volumes and motor and cognitive function tests.

Author Manuscript Author Manuscript Author Manuscript Author Manuscript

In conclusion, we analyzed spatially varying cerebellar patterns with respect to baseline age, follow-up interval, and sex in non-demented subjects older than 50 years. The results show that both age differences and longitudinal declines in regional cerebellar volumes. The effects of age and aging vary across subregions. Additionally, longitudinal changes can depend on baseline age and sex. Our findings can help to further understand the trajectories of cerebellum changes during normal aging and provide a normative standard against which effects of disease can be measured.

Supplementary Material

Refer to Web version on PubMed Central for supplementary material.

Acknowledgments

The author would thank to BLSA participants, colleagues of the Laboratory of Behavioral Neuroscience and Image Analysis and Communications Laboratory, and the staff of the Johns Hopkins and NIA MRI facilities.

This study was supported in part by the Intramural Research Program, National Institute on Aging, NIH.

References

Armstrong NM, An Y, Beason-Held L, Doshi J, Erus G, Ferrucci L, Davatzikos C, Resnick SM, 2019. Predictors of neurodegeneration differ between cognitively normal and subsequently impaired older adults. Neurobiol. Aging 75, 178–186. [PubMed: 30580127]

Bernard JA, Leopold DR, Calhoun VD, Mittal VA, 2015. Regional cerebellar volume and cognitive function from adolescence to late middle age. Hum. Brain Mapp. 36, 1102–1120. [PubMed: 25395058]

Bernard JA, Seidler RD, 2013. Relationships between regional cerebellar volume and sensorimotor and cognitive function in young and older adults. Cerebellum 12, 721–737. [PubMed: 23625382]

Bretz F, Hothorn T, Westfall P, 2011. Multiple Comparisons Using R. Chapman and Hall/CRC, New York.

Carass A, Cuzzocreo JL, Han S, Hernandez-Castillo CR, Rasser PE, Ganz M, Beliveau V, Dolz J, Ayed IB, Desrosiers C, et al. , 2018. Comparing fully automated state-of-the-art cerebellum parcellation from magnetic resonance images. Neuroimage 183, 150–172. [PubMed: 30099076]

Diedrichsen J, Balsters JH, Flavell J, Cussans E, Ramnani N, 2009. A probabilistic MR atlas of the human cerebellum. Neuroimage 46, 39–46. [PubMed: 19457380]

Doshi J, Erus G, Ou Y, Gaonkar B, Davatzikos C, 2013. Multi-atlas skull-stripping. Acad. Radiol. 20, 1566–1576. [PubMed: 24200484]

Fonov V, Evans AC, Botteron K, Almli CR, McKinstry RC, Collins DL, Group BDC, et al. , 2011. Unbiased average age-appropriate atlases for pediatric studies. Neuroimage 54, 313–327. [PubMed: 20656036]

Goh JO, An Y, Resnick SM, 2012. Differential trajectories of age-related changes in components of executive and memory processes. Psychol. Aging 27, 707–719. [PubMed: 22201331]

Guell X, Gabrieli JD, Schmahmann JD, 2018. Triple representation of language, working memory, social and emotion processing in the cerebellum: convergent evidence from task and seed-based resting-state fMRI analyses in a single large cohort. Neuroimage 172, 437–449. [PubMed: 29408539]

Han S, Carass A, He Y, Prince JL, 2020. Automatic cerebellum anatomical parcellation using U-Net with locally constrained optimization. Neuroimage 218, 116819.

Han S, He Y, Carass A, Ying SH, Prince JL, 2019. Cerebellum parcellation with convolutional neural networks. In: Angelini ED, Landman BA (Eds.), Medical Imaging 2019: Image Processing. International Society for Optics and Photonics, SPIE, pp. 143–148.

Author Manuscript Author Manuscript Author Manuscript Author Manuscript

Joo JWJ, Hormozdiari F, Han B, Eskin E, 2016. Multiple testing correction in linear mixed models. Genome Biol. 17, 62. [PubMed: 27039378]

Koo TK, Li MY, 2016. A guideline of selecting and reporting intraclass correlation coefficients for reliability research. J. Chiropract. Med. 15, 155–163.

Koppelmans V, Hoogendam YY, Hirsiger S, Mérillat S, Jäncke L, Seidler RD, 2017. Regional cerebellar volumetric correlates of manual motor and cognitive function. Brain Struct. Funct. 222, 1929–1944. [PubMed: 27699480]

Luft AR, Skalej M, Schulz JB, Welte D, Kolb R, Bürk K, Klockgether T, Voigt K, 1999. Patterns of age-related shrinkage in cerebellum and brainstem observed in vivo using three-dimensional MRI volumetry. Cerebr. Cortex 9, 712–721.

McCarrey AC, An Y, Kitner-Triolo MH, Ferrucci L, Resnick SM, 2016. Sex differences in cognitive trajectories in clinically normal older adults. Psychol. Aging 31, 166–175. [PubMed: 26796792]

Mottolese C, Richard N, Harquel S, Szathmari A, Sirigu A, Desmurget M, 2013. Mapping motor representations in the human cerebellum. Brain 136, 330–342. [PubMed: 22945964]

Park MTM, Pipitone J, Baer LH, Winterburn JL, Shah Y, Chavez S, Schira MM, Lobaugh NJ, Lerch JP, Voineskos AN, et al. , 2014. Derivation of high-resolution MRI atlases of the human cerebellum at 3 T and segmentation using multiple automatically generated templates. Neuroimage 95, 217–231. [PubMed: 24657354]

Pinheiro J, Bates D, DebRoy S, Sarkar D, R Core Team, 2019. Nlme: linear and nonlinear mixed effects models. URL: https://CRAN.R-project.org/package=nlme.Rpackage%20version3.1-140.

Raz N, Ghisletta P, Rodrigue KM, Kennedy KM, Lindenberger U, 2010. Trajectories of brain aging in middle-aged and older adults: regional and individual differences. Neuroimage 51, 501–511. [PubMed: 20298790]

Raz N, Lindenberger U, Rodrigue KM, Kennedy KM, Head D, Williamson A, Dahle C, Gerstorf D, Acker JD, 2005. Regional brain changes in aging healthy adults: general trends, individual differences and modifiers. Cerebr. Cortex 15, 1676–1689.

Raz N, Rodrigue KM, Kennedy KM, Dahle C, Head D, Acker JD, 2003. Differential age-related changes in the regional metencephalic volumes in humans: a 5-year follow-up. Neurosci. Lett. 349, 163–166. [PubMed: 12951194]

Raz N, Schmiedek F, Rodrigue KM, Kennedy KM, Lindenberger U, Lövdén M, 2013. Differential brain shrinkage over 6 months shows limited association with cognitive practice. Brain Cognit. 82, 171–180. [PubMed: 23665948]

Romero JE, Coupé P, Giraud R, Ta VT, Fonov V, Park MTM, Chakravarty MM, Voineskos AN, Manjón JV, 2017. CERES: a new cerebellum lobule segmentation method. Neuroimage 147, 916–924. [PubMed: 27833012]

Schmahmann JD, 2019. The cerebellum and cognition. Neurosci. Lett. 688, 62–75. [PubMed: 29997061]

Schmahmann JD, Doyon J, Petrides M, Evans AC, Toga AW, 2000. MRI Atlas of the Human Cerebellum. Academic Press, San Diego, CA.

Shock NW, Greulich RC, Costa PT Jr., Andres R, Lakatta EG, Arenberg D, Tobin JD, 1984. Normal Human Aging: the Baltimore Longitudinal Study of Aging. US Government Printing Office, Washington, DC.

Steele CJ, Chakravarty MM, 2018. Gray-matter structural variability in the human cerebellum: lobule-specific differences across sex and hemisphere. Neuroimage 170, 164–173. [PubMed: 28461060]

Stoodley CJ, Schmahmann JD, 2018. Functional topography of the human cerebellum. Handb. Clin. Neurol. 154, 59–70. [PubMed: 29903452]

Tian Q, Chastan N, Bair WN, Resnick SM, Ferrucci L, Studenski SA, 2017. The brain map of gait variability in aging, cognitive impairment and dementia—a systematic review. Neurosci. Biobehav. Rev. 74, 149–162. [PubMed: 28115194]

Tiemeier H, Lenroot RK, Greenstein DK, Tran L, Pierson R, Giedd JN, 2010. Cerebellum development during childhood and adolescence: a longitudinal morphometric MRI study. Neuroimage 49, 63–70. [PubMed: 19683586]

Tustison NJ, Avants BB, Cook PA, Zheng Y, Egan A, Yushkevich PA, Gee JC, 2010. N4ITK: improved N3 bias correction. IEEE Trans. Med. Imag. 29, 1310–1320.

Author Manuscript Author Manuscript Author Manuscript Author Manuscript

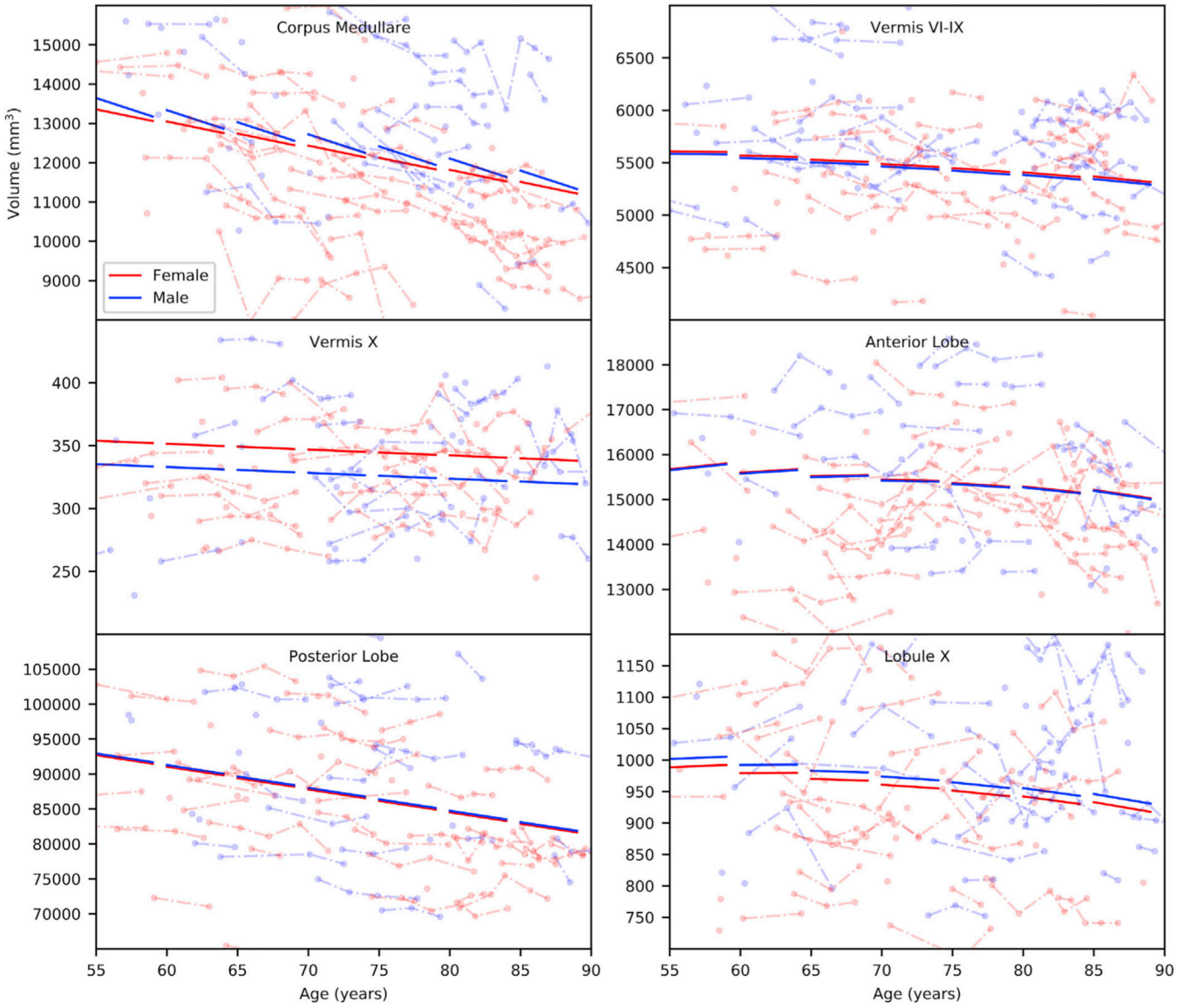

Fig. 1.

Example fitted population average trajectories by sex. Thick lines indicate the trajectories. Dots indicate volumes of randomly selected subjects and are connected by thin lines for the same subjects. Each thick line segment is plotted with the baseline age at its starting point, 0–4 follow-up years, and 1,400 cm^3 ICV.

Author Manuscript Author Manuscript Author Manuscript Author Manuscript

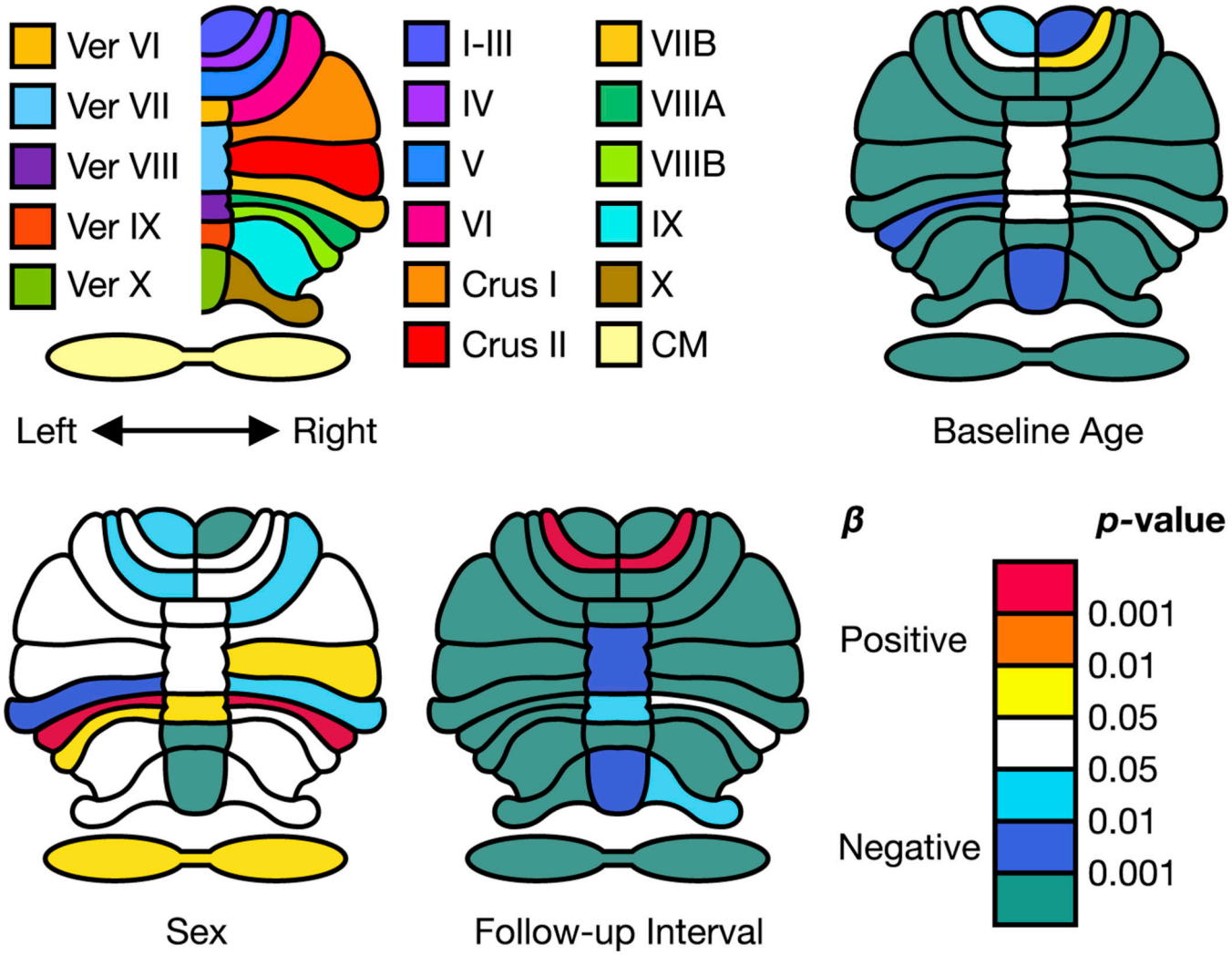

Fig. 2.

Raw *p*-values of baseline age, sex, and follow-up interval for each region. **Anterior Lobe** includes Lobules I–III, IV, and V, **Posterior Lobe** includes Lobule VI, Crus I, Crus II, and Lobules VIIB, VIIIA, VIIIB, and IX, and **Flocculonodular Lobe** includes Lobule X. **Ver:** Vermis. **CM:** Corpus Medullare.*β*: Fixed coefficients.

Author Manuscript Author Manuscript Author Manuscript Author Manuscript

Table 1

Literature summary. Conclusions include the findings of regional differences with respect to sex and age. **F:** female and **M:** male.

	No. subjects (F/M)	Age in years	Parcellation algorithm	Analysis type	No. regions	Conclusions
Luft et al. (1999)	48 (22/26)	19.8–73.1	semi-automated	cross-sectional	11	Larger volumes of Vermis VI–VII and Superior Posterior Lobe in female than male. Reduced volume with older age in vermis.
Tiemeier et al. (2010)	50 (25/25)	5–24	semi-automated	longitudinal	11	Different development trajectories of bilateral Superior Posterior and Inferior Posterior Lobes between male and female.
Bernard and Seidler (2013)	31 (8/23), 23 (14/9)	65.03±6.42, 22.04±3.47	SUIT (Diedrichsen et al., 2009)	cross-sectional	27	Reduced volumes with older age in bilateral Lobules I–IV, V, VI, and Crus I, and Left Crus II, and Vermis VI and VIIb.
Bernard et al. (2015)	123 (46/77)	12–65	SUIT (Diedrichsen et al., 2009)	cross-sectional	7	Volumes of different regions can be modeled differently using linear, logarithmic, or quadratic fitting with respect to age.
Koppelmans et al. (2017)	213 (112/101)	64–87	SUIT (Diedrichsen et al., 2009)	cross-sectional	11	Reduced volume loss with older age in bilateral Lobules I–VI, Crus I, and VIIIB–IX, Left Crus II–Lobule VIIB, and Vermis.
Steele and Chakravarty (2018)	327 (193/134)	22–36	MAGeT Brain (Park et al., 2014)	cross-sectional	33	Larger volumes in bilateral Crus II and Vermis VI for female and larger volumes in Right Lobules V, bilateral Lobules and Vermis VIIIA and VIIIB for male.

Neuroimage. Author manuscript; available in PMC 2023 November 28.

Author Manuscript

Author Manuscript

Author Manuscript

Author Manuscript

Table 2

Exclusion criteria.

Reason	No. subjects	No. images
Failed MNI alignment	14	30
Failed inhomogeneity correction	1	1
Failed parcellation	18	27
Image artifacts	12	12

Author Manuscript

Author Manuscript

Author Manuscript

Author Manuscript

Table 3

Sample characteristics. Follow-up intervals are calculated for subjects with two or more visits.

	Overall	Female	Male
Number of subjects	822	454	368
Number of visits	2,023	1,136	887
Age (years)			
Mean (SD)	70.7 (10.2)	69.8 (10.0)	72.0 (10.3)
Range	50.1–95.1	50.1–95.1	50.8–94.7
Follow-up (years)			
Mean (SD)	3.7 (1.9)	3.8 (1.9)	3.5 (1.9)
Range	0.8–9.3	0.8–9.3	0.8–9.0
ICV (cm^3)			
Mean (SD)	1,388.12 (140.20)	1,309.58 (105.96)	1,485.02 (114.32)
Range	999.75–1,886.29	999.75–1,672.97	1,216.47–1,886.29
Number of subjects by the total number of visits			
1	285	159	126
2	183	92	91
3	167	93	74
4	110	65	45
5	53	30	23
6	10	7	3
7	8	4	4
8	4	2	2
9	2	2	0

Author Manuscript Author Manuscript Author Manuscript Author Manuscript

Table 4

ICCs of cerebellar regions.

Region	ICC	Region	ICC
Corpus Medullare	0.96	**Vermis VI**	0.96
Vermis VII	0.96	**Vermis VIII**	0.98
Vermis IX	0.95	**Vermis X**	0.94
Left Lobules I–III	0.94	**Right Lobules I–III**	0.95
Left Lobule IV	0.90	**Right Lobule IV**	0.87
Left Lobule V	0.89	**Right Lobule V**	0.89
Left Lobule VI	0.97	**Right Lobule VI**	0.97
Left Crus I	0.96	**Right Crus I**	0.97
Left Crus II	0.92	**Right Crus II**	0.93
Left Lobule VIIB	0.93	**Right Lobule VIIB**	0.91
Left Lobule VIIIA	0.94	**Right Lobule VIIIA**	0.94
Left Lobule VIIIB	0.93	**Right Lobule VIIIB**	0.95
Left Lobule IX	0.99	**Right Lobule IX**	0.99
Left Lobule X	0.95	**Right Lobule X**	0.94

Author Manuscript Author Manuscript Author Manuscript Author Manuscript

Table 5

Fixed effect coefficients (β), standard errors (SE), and raw p values (p) for baseline age (Age), sex, follow-up interval (Time), and the interactions. Significant (Bonferroni adjusted $p \leq 0.05$) effects are highlighted. **AL:** Anterior Lobe. **CM:** Corpus Medullare. **H:** Hemisphere. **PL:** Posterior Lobe. **L:** left. **R:** right. **Ver:** Vermis.

	Age			**Sex**			**Time**			**Age × Time**			**Sex × Time**		
	β	**SE**	p	β	**SE**	p	β	**SE**	p	β	**SE**	p	β	**SE**	p
Total	**−414.30**	**31.60**	**9×10^{-36}**	464.25	824.05	6×10^{-1}	**−419.73**	**20.78**	**3×10^{-78}**	**−7.75**	**2.22**	**5×10^{-4}**	−82.24	41.16	5×10^{-2}
CM	**−61.54**	**4.82**	**3×10^{-34}**	287.43	125.88	2×10^{-2}	**−95.71**	**4.93**	**4×10^{-73}**	−0.21	0.53	7×10^{-1}	**−43.38**	**9.80**	**1×10^{-5}**
L H	**−178.93**	**13.95**	**2×10^{-34}**	15.13	363.53	1×10^{0}	**−188.24**	**10.49**	**6×10^{-64}**	**−4.69**	**1.12**	**3×10^{-5}**	−26.01	20.78	2×10^{-1}
R H	**−164.86**	**13.98**	**1×10^{-29}**	204.96	364.43	6×10^{-1}	**−129.00**	**10.55**	**2×10^{-32}**	−3.01	1.13	8×10^{-3}	−18.72	20.96	4×10^{-1}
Ver	**−8.49**	**1.79**	**2×10^{-6}**	−42.61	46.74	4×10^{-1}	**−7.67**	**1.14**	**2×10^{-11}**	**−0.42**	**0.12**	**5×10^{-4}**	−2.03	2.26	4×10^{-1}
Ver VI−IX	**−8.02**	**1.73**	**4×10^{-6}**	−23.95	45.27	6×10^{-1}	**−7.20**	**1.11**	**1×10^{-10}**	**−0.39**	**0.12**	**1×10^{-3}**	−2.32	2.20	3×10^{-1}
Ver VI	**−4.85**	**0.69**	**5×10^{-12}**	−19.28	18.03	3×10^{-1}	**−1.72**	**0.46**	**2×10^{-4}**	**−0.23**	**0.05**	**2×10^{-6}**	0.34	0.91	7×10^{-1}
Ver VII	−0.16	0.57	8×10^{-1}	−15.41	14.94	3×10^{-1}	−1.18	0.43	6×10^{-3}	−0.09	0.05	5×10^{-2}	−1.56	0.85	7×10^{-2}
Ver VIII	−0.22	0.98	8×10^{-1}	61.19	25.54	2×10^{-2}	−1.28	0.58	3×10^{-2}	−0.10	0.06	1×10^{-1}	−0.84	1.15	5×10^{-1}
Ver IX	**−2.79**	**0.47**	**4×10^{-9}**	**−49.43**	**12.21**	**6×10^{-5}**	**−2.94**	**0.43**	**1×10^{-11}**	0.03	0.05	5×10^{-1}	0.11	0.85	9×10^{-1}
Ver X	−0.46	0.17	7×10^{-3}	**−18.53**	**4.45**	**3×10^{-5}**	−0.48	0.16	2×10^{-3}	−0.03	0.02	6×10^{-2}	0.32	0.31	3×10^{-1}
L AL	−4.68	2.84	1×10^{-1}	−94.32	73.79	2×10^{-1}	2.35	2.82	4×10^{-1}	**−1.09**	**0.30**	**3×10^{-4}**	**19.47**	**5.61**	**5×10^{-4}**
R AL	**−10.72**	**2.78**	**1×10^{-4}**	75.46	72.20	3×10^{-1}	**−9.58**	**2.74**	**5×10^{-4}**	**−1.45**	**0.29**	**9×10^{-7}**	4.33	5.45	4×10^{-1}
L I−III	−1.45	0.63	2×10^{-2}	−37.04	16.37	2×10^{-2}	**−3.09**	**0.61**	**6×10^{-7}**	−0.14	0.07	3×10^{-2}	−0.03	1.22	1×10^{0}
R I−III	**−2.10**	**0.64**	**1×10^{-3}**	**−56.46**	**16.72**	**8×10^{-4}**	**−3.55**	**0.55**	**2×10^{-10}**	−0.10	0.06	1×10^{-1}	−0.75	1.10	5×10^{-1}
L IV	2.87	1.81	1×10^{-1}	15.85	46.78	7×10^{-1}	**17.66**	**2.23**	**5×10^{-15}**	−0.62	0.24	1×10^{-2}	13.47	4.44	2×10^{-3}
R IV	4.36	1.78	1×10^{-2}	82.54	46.10	7×10^{-2}	**13.93**	**2.58**	**8×10^{-8}**	**−0.89**	**0.28**	**1×10^{-3}**	11.09	5.14	3×10^{-2}
L V	**−6.10**	**1.41**	**2×10^{-5}**	−71.96	36.62	5×10^{-2}	**−12.38**	**2.02**	**1×10^{-9}**	−0.26	0.22	2×10^{-1}	5.44	4.01	2×10^{-1}
R V	**−13.01**	**1.47**	**5×10^{-18}**	48.12	37.56	2×10^{-1}	**−19.44**	**1.88**	**4×10^{-24}**	−0.37	0.20	7×10^{-2}	−5.39	3.74	1×10^{-1}
L PL	**−173.36**	**12.69**	**2×10^{-38}**	104.39	330.19	8×10^{-1}	**−188.69**	**10.17**	**1×10^{-67}**	−3.42	1.09	2×10^{-3}	−44.29	20.16	3×10^{-2}
R PL	**−153.41**	**12.62**	**2×10^{-31}**	128.18	328.77	7×10^{-1}	**−118.54**	**10.13**	**5×10^{-30}**	−1.34	1.09	2×10^{-1}	−20.05	20.12	3×10^{-1}
L VI	**−40.33**	**4.03**	**2×10^{-22}**	−125.73	104.76	2×10^{-1}	**−55.64**	**2.78**	**3×10^{-77}**	−0.80	0.30	7×10^{-3}	**−18.07**	**5.51**	**1×10^{-3}**
R VI	**−30.80**	**3.91**	**1×10^{-14}**	−246.55	101.80	2×10^{-2}	**−37.31**	**2.70**	**3×10^{-40}**	−0.15	0.29	6×10^{-1}	−1.27	5.37	8×10^{-1}

Neuroimage. Author manuscript; available in PMC 2023 November 28.

Author Manuscript Author Manuscript Author Manuscript Author Manuscript

	Age			Sex			Time			Age × Time			Sex × Time		
	β	SE	p	β	SE	p	β	SE	p	β	SE	p	β	SE	p
L Crus I	**−59.69**	**5.44**	**3×10^{-26}**	−189.04	141.08	2×10^{-1}	**−47.36**	**4.33**	**1×10^{-26}**	−1.43	0.46	2×10^{-3}	−4.74	8.59	6×10^{-1}
R Crus I	**−57.88**	**5.51**	**3×10^{-24}**	−10.81	143.77	9×10^{-1}	**−22.14**	**4.53**	**1×10^{-6}**	−0.33	0.49	5×10^{-1}	−3.20	9.01	7×10^{-1}
L Crus II	**−22.04**	**3.74**	**6×10^{-9}**	181.57	97.28	6×10^{-2}	**−25.85**	**3.72**	**6×10^{-12}**	−0.43	0.40	3×10^{-1}	−20.66	7.38	5×10^{-3}
R Crus II	**−19.16**	**3.99**	**2×10^{-6}**	228.66	103.56	3×10^{-2}	**−17.27**	**3.92**	**1×10^{-5}**	−0.13	0.42	8×10^{-1}	**−27.04**	**7.78**	**5×10^{-4}**
L VIIB	**−27.93**	**3.10**	**1×10^{-18}**	−234.96	80.07	3×10^{-3}	**−27.45**	**3.04**	**6×10^{-19}**	0.14	0.32	7×10^{-1}	10.69	6.02	8×10^{-2}
R VIIB	**−27.73**	**3.11**	**3×10^{-18}**	−203.93	80.09	1×10^{-2}	**−30.98**	**3.33**	**7×10^{-20}**	−0.42	0.36	2×10^{-1}	16.76	6.62	1×10^{-2}
L VIIIA	−8.93	2.88	2×10^{-3}	**419.85**	**75.10**	**3×10^{-8}**	**−11.19**	**3.20**	**5×10^{-4}**	−0.48	0.34	2×10^{-1}	−2.67	6.36	7×10^{-1}
R VIIIA	−0.22	2.45	9×10^{-1}	**348.53**	**63.42**	**5×10^{-8}**	3.71	2.85	2×10^{-1}	−0.05	0.31	9×10^{-1}	−11.15	5.67	5×10^{-2}
L VIIIB	**−6.65**	**1.96**	**7×10^{-4}**	110.22	50.48	3×10^{-2}	**−8.65**	**1.89**	**5×10^{-6}**	−0.35	0.20	9×10^{-2}	−0.78	3.76	8×10^{-1}
R VIIIB	**−10.84**	**1.92**	**2×10^{-8}**	74.30	49.95	1×10^{-1}	**−7.12**	**1.70**	**3×10^{-5}**	−0.24	0.18	2×10^{-1}	1.47	3.38	7×10^{-1}
L IX	**−7.89**	**2.06**	**1×10^{-4}**	−42.45	53.72	4×10^{-1}	**−9.69**	**0.83**	**6×10^{-30}**	−0.07	0.09	4×10^{-1}	−3.98	1.65	2×10^{-2}
R IX	**−6.74**	**2.03**	**9×10^{-4}**	−41.60	52.82	4×10^{-1}	**−8.05**	**0.92**	**5×10^{-18}**	−0.15	0.10	1×10^{-1}	−0.76	1.82	7×10^{-1}
L X	**−1.02**	**0.24**	**2×10^{-5}**	10.22	6.13	1×10^{-1}	**−0.99**	**0.23**	**2×10^{-5}**	−0.07	0.02	6×10^{-3}	−0.08	0.46	9×10^{-1}
R X	**−0.84**	**0.23**	**3×10^{-4}**	2.70	6.04	7×10^{-1}	−0.48	0.22	3×10^{-2}	**−0.09**	**0.02**	**3×10^{-4}**	−1.10	0.44	1×10^{-2}

Neuroimage. Author manuscript; available in PMC 2023 November 28.